ELSEVIER

Nuclear Physics B 482 [FS] (1996) 639–659

NUCLEAR PHYSICS B [FS]

Excited states by analytic continuation of TBA equations

Patrick Dorey [1], Roberto Tateo [2]

Department of Mathematical Sciences, University of Durham, Durham DH1 3LE, UK

Received 29 July 1996; accepted 16 September 1996

Abstract

We suggest an approach to the problem of finding integral equations for the excited states of an integrable model, starting from the thermodynamic Bethe ansatz equations for its ground state. The idea relies on analytic continuation through complex values of the coupling constant, and an analysis of the monodromies that the equations and their solutions undergo. For the scaling Lee–Yang model, we find equations in this way for the one- and two-particle states in the spin-zero sector, and suggest various generalisations. Numerical results show excellent agreement with the truncated conformal space approach, and we also treat some of the ultraviolet and infrared asymptotics analytically.

PACS: 05.50+q; 11.25.Hf; 64.60.Ak; 75.10.Hk

1. Introduction

The thermodynamic Bethe ansatz (TBA) [1] has proved to be a very useful tool in the study of integrable two-dimensional field theories. The finite-volume ground-state energy can now be found for many models, expressed in each case in terms of the solution of a set of non-linear integral equations. These turn out to be vulnerable to both numerical and analytical attack, and yield a large amount of non-trivial information. Given these successes, it is natural to hope that similar equations might describe the remaining energy levels. However, the derivation of the TBA equations relies on arguments which perforce single out the ground state, and, save for a few states which become degenerate

[1] E-mail: P.E.Dorey@durham.ac.uk

[2] E-mail: Roberto.Tateo@durham.ac.uk

PII S0550-3213(96)00516-0

with the ground state in large volumes [2–4], the desired generalisation has proved elusive.

In this paper we propose to sidestep the problem by returning to the old idea that one can move between energy levels by analytic continuation in a suitable parameter. In 0+1 dimensions, the quantum-mechanical problem, this was seen most spectacularly in the analysis of the quantum anharmonic oscillator performed by Bender and Wu [5]. Somewhat simpler in analytic structure, but more relevant to the following, is the finite volume spectrum of the Ising field theory in 1+1 dimensions. If the 'spatial' dimension is rolled up into a circle of circumference R, then the ground-state energy (the lowest eigenvalue of the infinitesimal transfer matrix in the 'time' direction) can be written as [6]

$$E_0^{\mathrm{IM}}(M,R) = E_{\mathrm{bulk}}^{\mathrm{IM}}(M,R) - \frac{\pi}{6R} c_0^{\mathrm{IM}}(MR)\,, \tag{1.1}$$

where M the inverse of the bulk correlation length, $E_{\mathrm{bulk}}^{\mathrm{IM}}(M,R)$ contains the (as it happens logarithmically divergent) bulk contribution, and

$$c_0^{\mathrm{IM}}(r) = \frac{1}{2} - \frac{3r^2}{2\pi^2}\left[\log\frac{1}{r} + \frac{1}{2} + \ln\pi - \gamma_E\right] + \frac{6}{\pi}\sum_{k=1}^{\infty}\left(\sqrt{r^2+(2k-1)^2\pi^2} - (2k-1)\pi - \frac{r^2}{2(2k-1)\pi}\right) \tag{1.2}$$

with $r = MR$ and $\gamma_E = 0.57721566\ldots$ Apart from the logarithmic singularity at $R = 0$, this exhibits a series of square root branch cuts, evenly spaced along the imaginary axis. Suppose that R is continued into the complex plane along a path enclosing the singularities at $k = k_1, k_2, \ldots, k_n$. Then on its return to the real axis, $E_0^{\mathrm{IM}}(M,R)$ has been replaced by

$$E_{k_1,k_2\ldots k_n}^{\mathrm{IM}}(M,R) = E_0^{\mathrm{IM}}(M,R) + \frac{2}{R}\sum_{i=1}^{n}\sqrt{r^2+(2k_i-1)^2\pi^2}\,, \tag{1.3}$$

an excited state with ultraviolet scaling dimension $\sum_i(2k_i-1)$. This covers all of the symmetrical descendants of the primary fields I and ε in the spin-zero sector. To find descendants of the spin field σ, the same process can be repeated, but this time starting from the lowest excited state in the low-temperature regime, which degenerates with E_0 in infinite volume and is accessible as the ground state with twisted boundary conditions (see for example Ref. [4]).

In more general situations explicit expressions such as (1.1), (1.2) are not available. Even for integrable perturbations of conformal field theories, the best one can do is to express the ground-state energy in terms of the solutions $\varepsilon_a(\theta)$ to a set of TBA equations. The simplest case is the scaling Lee–Yang model, or SLYM. This field theory, a perturbation of the non-unitary minimal model $\mathcal{M}(2/5)$ by its unique relevant operator φ, has the action

$$\mathcal{A}_{\mathrm{SLYM}} = \mathcal{A}_{\mathcal{M}(2/5)} + \imath\lambda\int\varphi(x)d^2x\,. \tag{1.4}$$

With $M(\lambda) = (2.642944\ldots)\lambda^{5/12}$ [7] and $r = M(\lambda)R$, the single TBA equation reads [1]

$$\varepsilon(\theta) = r\cosh\theta - \phi * L(\theta)\,, \tag{1.5}$$

where

$$L(\theta) = \log\left(1 + e^{-\varepsilon(\theta)}\right)\,, \qquad f*g(\theta) = \frac{1}{2\pi}\int_{-\infty}^{\infty} d\theta' f(\theta-\theta')g(\theta')\,, \tag{1.6}$$

and

$$\phi(\theta) = -\imath\frac{\partial}{\partial\theta}\log S(\theta)\,, \qquad S(\theta) = \frac{\sinh(\theta) + \imath\sin(\pi/3)}{\sinh(\theta) - \imath\sin(\pi/3)}\,. \tag{1.7}$$

The function $S(\theta)$ is the S-matrix of the single neutral particle in the model [8], and has the 'ϕ^3' bootstrap property, that $S(\theta-\imath\pi/3)S(\theta+\imath\pi/3) = S(\theta)$. In terms of these quantities, the ground-state energy is

$$E_0(\lambda, R) = E_{\text{bulk}}(\lambda, R) - \frac{\pi}{6R}c_0(r) \tag{1.8}$$

with

$$E_{\text{bulk}}(\lambda, R) = \frac{-M(\lambda)^2}{4\sqrt{3}}R\,, \qquad c_0(r) = \frac{3}{\pi^2}\int_{-\infty}^{\infty} d\theta\, r\cosh\theta L(\theta)\,. \tag{1.9}$$

At first sight (1.5)–(1.9) are very different from (1.1), (1.2), and it is not clear that analytic continuation will be practicable. To get a clue as to how to proceed, return to (1.2) and consider its alternative integral representation

$$c_0^{\text{IM}}(r) = \frac{3}{\pi^2}\int_{-\infty}^{\infty} d\theta\, r\cosh\theta\log\left(1+e^{-r\cosh\theta}\right)\,. \tag{1.10}$$

As r moves into the complex plane, a singularity in c_0^{IM} might be expected whenever $1+e^{-r\cosh\theta_0} = 0$ for some real θ_0. However, deforming the contour of integration away from the real axis near θ_0 shows that such impressions are generally deceptive. This manœuvre would only fail if two singularities were to approach the real axis from opposite sides, trapping the contour. This gives rise to a so-called 'pinch singularity', usually a branch point. If r is continued along some path encircling the critical value, the two θ-singularities (in this case, singularities in $\log(1+e^{-r\cosh\theta})$) execute a little dance in the complex plane (here, they just swap over), after which the contour has become tangled up. Undoing the tangle gives rise to the discontinuity across the cut. All of this is very clearly explained in chapter 2 of the book by Eden et al. [9], and here we simply remark that it is an instructive exercise to recover the results already quoted by the use of such methods.

For more general TBA systems, life is complicated by the replacement of $r\cosh\theta$ by $\varepsilon(\theta)$, a function which may itself be subject to non-trivial monodromies. Furthermore,

$\varepsilon(\theta)$ is not known explicitly even for the ground state. Fortunately, only qualitative, 'topological', information about the movement of singularities is needed in order to deduce the modified TBA equations, and for this numerical work will suffice.

2. One-particle states

Both the truncated conformal space approach (TCSA) [10], and the numerical extrapolation of TBA results found for $\lambda \in \mathbb{R}^+$, have led to the conclusion that the ground-state energy of the SLYM has a square root singularity at $R(-\lambda)^{5/12} \approx 1.1325$. In fact, this can also be seen directly from the initial TBA system (1.5). For this it is convenient to adsorb the bulk term into $c_0(r)$, and work instead with the ground-state scaling function $F_0(r)$:

$$E_0(\lambda, R) = \frac{2\pi}{R} F_0(r) , \qquad F_0(r) = -\frac{r^2}{8\sqrt{3}\pi} - \frac{1}{12} c_0(r) . \tag{2.1}$$

The function F_0 thus defined is expected to be a regular function of $r^{12/5}$ [11], well-suited to analytic continuation. Negative values of λ put r on the ray $r = \rho e^{5\pi i/12}$, $\rho \in \mathbb{R}^+$. A suitably damped numerical iteration of the TBA equation (1.5) is convergent along this line, and the resulting ground-state scaling function turns out to be real out to $\rho = \rho_0 \approx 2.99315$, there being clear evidence for a square-root singularity at this point. This is shown in the lower set of points in Fig. 1, and matches in all aspects the TCSA results found earlier by Yurov and Zamolodchikov [10]. We conclude that the TBA is able to provide reliable (and, indeed, highly accurate) information even away from real values of r.

Next, the idea is to circle around the singularity, in the hope of picking up the next branch of the function – the first excited state. Analytic continuation is straightforwardly implemented when solving the TBA iteratively, by varying r step by step and at each new value of r taking the initial iterate $\varepsilon^{(0)}$ to be the final iterate $\varepsilon^{(n)}$ of the previous step. The steps in r must not be too large, or the solution being tracked may be lost. Also, one must guard against numerical instabilities which are purely artifacts of the iteration scheme. We adopted the simplest possible option, iterating as

$$\varepsilon^{(n+1)}(\theta) = a \left[r \cosh\theta - \phi * L^{(n)}(\theta) \right] + (1-a)\varepsilon^{(n)}(\theta) , \tag{2.2}$$

and finding empirically that values of a between 0.5 and 0.05 (depending on the value of r) gave optimal results. Stability rather than efficiency turns out to be the key issue, and it is worth seeking a more sophisticated approach. Nevertheless, (2.2) was adequate for the current work.

Of more profound import are the changes needed should a singularity of $L(\theta)$ cross the real axis. In such a situation, further analytic continuation results in a function ε which solves a modified TBA equation, with the contour of integration diverted away from its original track long enough to avoid the singularity. To check for this, we must locate the complex zeroes and poles in $z(\theta) \equiv 1 + e^{-\varepsilon(\theta)}$, and be on our guard

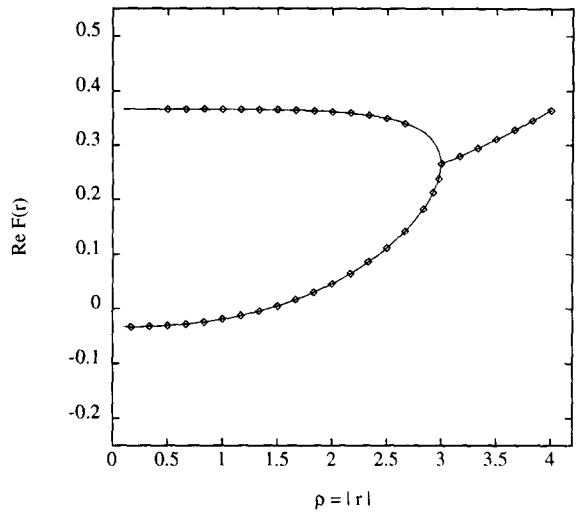

Fig. 1. Two solutions to the basic TBA equation on the negative-λ line (points) versus TCSA data (continuous lines).

whenever any of them venture too close to the real axis. This is easily done, at least numerically – once $\varepsilon(\theta)$ is known along the real axis (or along some more general contour), Eq. (1.5) provides an integral representation which can be used to reconstruct the function everywhere. The only point to watch is that the singularities of ϕ at $\pm\imath\pi/3$ and beyond necessitate the introduction of extra terms when $\varepsilon(\theta)$ is continued beyond the strip $-\imath\pi/3 < \mathrm{Im}(\theta) < \imath\pi/3$.

Near the real axis at large values of $|\mathrm{Re}(\theta)|$, the $r\cosh\theta$ term comes to dominate (1.5), and so two series of zeroes in $z(\theta)$ are always seen, approaching the two half lines $\pm\{\theta \in \mathbb{C} : \mathrm{Re}(\theta) > 0, \mathrm{Im}(\theta) = [\pi/2 - \mathrm{Arg}(r)]\}$. However, if r lies on the initial segment of the negative-λ line, $\mathrm{Arg}(r) = 5\pi/12$ and $0 < |r| < \rho_0$, we found evidence that, for the solution just discussed, a stronger result holds: up to our numerical accuracy, all of the zeroes in a strip along the real axis have imaginary part *exactly* equal to $\pm\pi/12$. As $|r| = \rho \to 0$, the zeroes on the upper half line slide off towards $+\infty$, while those on the lower head for $-\infty$. The pattern becomes that of a pair of kink systems, one starting near $\theta = -\log(1/r)$, the other near $\theta = +\log(1/r)$. Conversely, as $\rho \to \rho_0$, the two sets approach each other, although they always remain in their respective left and right halves of the complex plane.

If r is continued in an anticlockwise sense about the critical point and back to the negative-λ line, it turns out that *none* of these zeroes cross the real axis. The original TBA system (1.5) continues to hold, but its solution $\varepsilon(\theta)$ has nevertheless undergone a non-trivial monodromy. The values of the scaling function which result form the upper set of points in Fig. 1, and match perfectly with the TCSA data for the first excited state, at least in the range of ρ for which our rather crude iteration scheme is stable. Hence the TBA equation (1.5) is at least doubly degenerate along the negative-λ line, with the second solution as physically relevant as the first. The monodromy has an interesting

effect on the pattern of zeroes of $z(\theta)$: while their imaginary parts apparently remain at $\pm\pi/12$, their real parts are no longer so simply arranged, at least for ρ smaller than about 2.8. The rightmost zero on the lower half line moves into the right half plane $\mathrm{Re}(\theta) > 0$, thus lying to the right of the leftmost zero on the upper half line – the left and right kink systems have become entwined, a feature that persists even as the two systems try to split apart in the $\rho \to 0$ limit. On the other hand, as ρ increases past 2.8, the ordering is briefly restored, though there does not seem to be any great significance to this fact. Our numerics for the upper branch quickly become unstable in this region, but an extrapolation of the positions of the errant pair of zeroes is consistent with their moving continuously to the same positions ($\approx \pm(0.24+\imath\pi/12)$) as found for the first two zeroes on the lower branch, as $\rho \to \rho_0$. This supports our supposition that the basic TBA system describes the first excited state on the whole segment $0 < \rho < \rho_0$, and not just on that part where our iterations converged.

Having found this excited state for r on the negative-λ line, we now continue r back to the real axis. As $\mathrm{Arg}(r)$ decreases from $5\pi/12$, all of the zeroes of $z(\theta)$ bar the first on the upper half line start to move up, towards the line $\mathrm{Im}(\theta) = \pi/2$. The first zero, on the other hand, is observed to move down, towards the real axis. The zeroes on the lower half line behave in a symmetrical fashion, as indeed they must given the $\theta \to -\theta$ symmetry of the basic equations. This is precisely the situation mentioned above, and we should be ready to modify the TBA equations when the two singularities actually hit the axis. Unfortunately the iterative solution of the equation becomes unstable when singularities in $L(\theta)$ get too close to the integration contour. It is possible to get a little further by distorting the contour along which the equations are being solved; in any event, a Padé extrapolation of the positions of the two singularities under suspicion clearly showed them crossing the real axis as $\mathrm{Arg}(r)$ decreased. Assume that r is such that these two singularities in $L(\theta)$ *have* crossed the real axis, and now lie at $-\theta_0$, θ_0. (Here and in analogous situations later on, we adopt the convention that of the pair $\{-\theta_0, \theta_0\}$, it is θ_0 which has the positive imaginary part after the axis is crossed.) Coming in from the left, the integration contour for the convolution in (1.5) must now first loop down and around the singularity at $-\theta_0$, and then back up and over the singularity at $+\theta_0$, before proceeding to $+\infty$ along the real axis. An integration by parts turns these logarithmic singularities into simple poles; evaluating the residues then allows the equation to be recast with the contour running along the real axis again:

$$\varepsilon(\theta) = r\cosh\theta + \log\frac{S(\theta-\theta_0)}{S(\theta+\theta_0)} - \phi * L(\theta)\,. \tag{2.3}$$

Similarly, the expression for $F_0(r)$ is modified, with c_0 of Eq. (1.9) being replaced by

$$c(r) = \frac{12r}{\pi}\iota\sinh\theta_0 + \frac{3}{\pi^2}\int_{-\infty}^{\infty} d\theta\, r\cosh\theta L(\theta)\,. \tag{2.4}$$

Although these equations appear to contain an unknown parameter, namely θ_0, this is not the case: self-consistency demands that θ_0 coincide with the position of the singularity

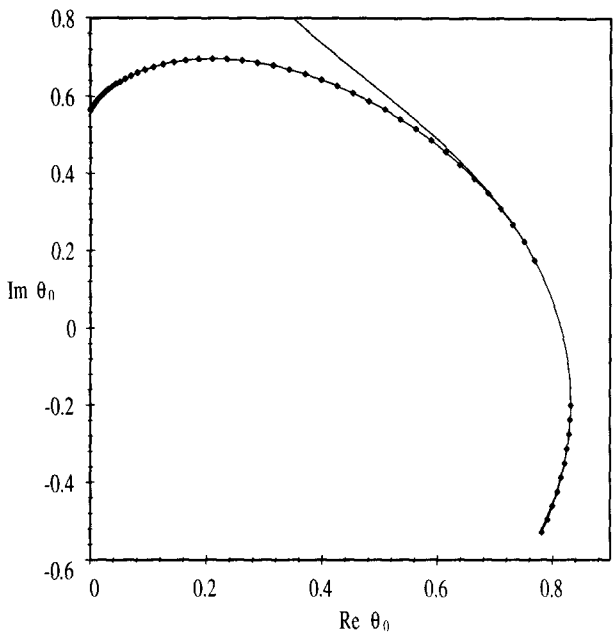

Fig. 2. Padé extrapolation of θ_0 for the first excited state, from $r = 1.5\imath$ (lower right) to $r = 4.5$ (upper left), and back.

in $L(\theta)$ that necessitated its introduction in the first place. In this case, this translates as $\varepsilon(\theta_0) = \imath\pi$ (the branch of the logarithm to choose here can be fixed by continuity, starting from the situation before the singularity crosses the axis). Substituting $\theta = \theta_0$ into (2.3) then gives

$$0 = r\cosh\theta_0 - \log S(2\theta_0) - \phi * L(\theta_0)\,. \tag{2.5}$$

Flipping between Eqs. (2.3) and (2.5), iterative schemes can be set up which are convergent in most regions of interest, given a reasonably accurate estimate of θ_0 for the initial iterate. Starting with the extrapolated singularities of the 'excited' solution to (1.5), a solution to (2.4) can be picked up and followed all the way back to the real r axis. In this way, we tracked a solution along the line $r = t + (1.5 - t/3)\imath$, with t varying from 0 to 4.5. Eq. (1.5) converged for t less than about 0.45, while (2.3) took over as soon as t became larger than 1. The problems for $0.45 < t < 1$ seem to be artifacts of our iteration schemes, and in particular the good agreement of the Padé-extrapolated singularity positions, both forwards and backwards, leave little doubt that the gap was crossed correctly. Fig. 2 matches these extrapolations (shown by the continuous lines) with a selection of points from the 'raw' data. Points in the lower half plane (before the singularity has crossed the axis) derive from the unmodified TBA system (1.5), and those in the upper half plane from the modified system (2.3). (For the backwards fit, where a greater range of t was available along which to collect data from which to extrapolate, the matching is so good that the discrepancies with the target points are rather hard to spot on the figure.) It is also possible to monitor the behaviour of $c(r)$,

finding good agreement with TCSA data in both regimes.

As r approaches the real axis, we see that θ_0 approaches $\imath(\pi/6+\delta(r))$, with $\delta(r)$ a small positive correction which tends to zero for large real r. This information is enough to pin down the large-r asymptotics of (2.5). As r grows, the convolution term becomes relatively small, and the first two terms must cancel between themselves. The only way this can happen as r grows is for $2\theta_0$ to approach a singularity of S; with $\theta_0 \sim \imath\pi/6$, the singularity at $\imath\pi/3$ is the relevant one. Substituting $\theta_0(r) \simeq \imath(\pi/6+\delta(r))$ and solving gives

$$\theta_0(r) \sim \imath\left(\pi/6+\sqrt{3}e^{-\sqrt{3}r/2}\right) . \tag{2.6}$$

This immediately tells us the leading asymptotic of $c(r)$: substituting (2.6) into first term in (2.4) gives $c(r) \sim -6r(1+3e^{-\sqrt{3}r/2})/\pi$. The next term is also easy to find, dropping the third factor in (2.3) and using the zeroth-order value of θ_0, namely $\imath\pi/6$, in order to find the leading behaviour of $\varepsilon(\theta)$ for substitution into (2.4). Gathering everything together we find

$$c(r) \sim \frac{-6r}{\pi}\left(1+3e^{-\sqrt{3}r/2}-\frac{1}{2\pi}\int_{-\infty}^{\infty} d\theta\,\cosh\theta\; S(\theta+\imath\pi/2)e^{-r\cosh\theta}\right) , \tag{2.7}$$

where for the last term the bootstrap relation $S(\theta+\imath\pi/6)/S(\theta-\imath\pi/6) = S(\theta+\imath\pi/2)$, relevant because θ_0 has been given its asymptotic value, was used to reduce the two S-matrices in (2.3) to one. This matches exactly with the asymptotics predicted in Refs. [10,12] for the spin-zero one-particle state, and therefore lends strong support to our proposal. Further evidence will come from the numerical comparisons with TCSA data to be reported shortly, but first we would like to mention a natural generalisation of Eqs. (2.3)–(2.5) which seems to capture all the remaining one-particle states.

The equations to consider read, for $r \in \mathbb{R}$, as follows:

$$\begin{aligned}
\varepsilon(\theta) &= r\cosh\theta + \log\frac{S(\theta-\theta_0)}{S(\theta-\overline{\theta}_0)} - \phi * L(\theta) ,\\
c(r) &= \imath\frac{6r}{\pi}(\sinh\theta_0 - \sinh\overline{\theta}_0) + \frac{3}{\pi^2}\int_{-\infty}^{\infty} d\theta\, r\cosh\theta L(\theta) ,
\end{aligned} \tag{2.8}$$

where θ_0, $\overline{\theta}_0$ are the complex-conjugate locations of a pair of singularities in $L(\theta)$. We will discuss the one-particle states with positive spin, and so we take $\mathrm{Re}(\theta_0) > 0$; the negative-spin states work similarly. The earlier equations at real values of r are recovered if θ_0 is forced to be purely imaginary; conversely if r were to become complex in (2.8), then θ_0 and $\overline{\theta}_0$ would generally cease to be complex conjugates, and would have to be tracked individually. Eq. (2.5) must also be modified, both because of the changed form of (2.8) and also to allow for a more general singularity at θ_0, namely $\varepsilon(\theta_0) = (2n+1)\pi\imath$ (and $n > 0$ for $\mathrm{Re}(\theta_0) > 0$). The equation becomes

$$2n\pi\imath = r\cosh\theta_0 - \log S(2\imath\mathrm{Im}(\theta_0)) - \phi * L(\theta_0) . \tag{2.9}$$

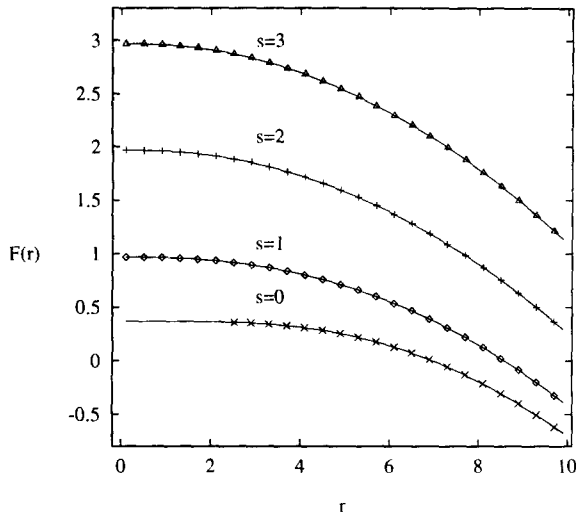

Fig. 3. Proposed one-particle scaling functions (points) compared with TCSA data (continuous lines).

Part of the motivation for these equations came from the form of the two-particle equations to be introduced in the next section; but to see immediately that they have a chance of being correct, consider the large-r asymptotics. The convolution term is subleading, and again it turns out that the balance between the first two terms is achieved via $\mathrm{Im}(\theta_0) = \pi/6 + \delta(r)$ with $\delta(r)$ vanishing as $r \to \infty$. Now take the imaginary part of (2.9) (previously this vanished automatically for real r), and consider its behaviour as r becomes large:

$$\begin{aligned} 2n\pi &= r \sinh(\mathrm{Re}(\theta_0)) \sin(\pi/6+\delta(r)) - \mathrm{Im} \log S(2\imath(\pi/6+\delta(r))) \\ &\sim \frac{r}{2} \sinh(\mathrm{Re}(\theta_0)) - \tfrac{1}{2}(1-\mathrm{sign}(\delta(r)))\pi . \end{aligned} \tag{2.10}$$

The term $\frac{1}{2}(1-\mathrm{sign}(\delta(r)))\pi$ is included to allow for $\delta(r)$ being negative, in which case $S(2\imath(\pi/6+\delta(r)))$ is negative and the logarithm picks up an imaginary part. Feeding this into (2.8) gives

$$c(r) \sim -\frac{6r}{\pi}\sqrt{1+(2\pi s/r)^2} \tag{2.11}$$

with $s = 2n + \frac{1}{2}(1-\mathrm{sign}(\delta(r)))$. This is exactly as expected for a one-particle state with spin s.

One final observation: for all but the spin-zero one-particle state, Eq. (2.8) is not symmetrical under $\theta \to -\theta$. Hence it can never be obtained by analytic continuation of the ground-state equation. But this is just as one would expect: the entire Hilbert space of the SLYM splits up into sectors of different spin, and analytic continuation can only ever move levels around within a given sector.

Fig. 3 compares the numerical solutions of Eqs. (2.3), (2.9) with TCSA data, for the first four one-particle levels. We used the TCSA program of Ref. [13], truncating

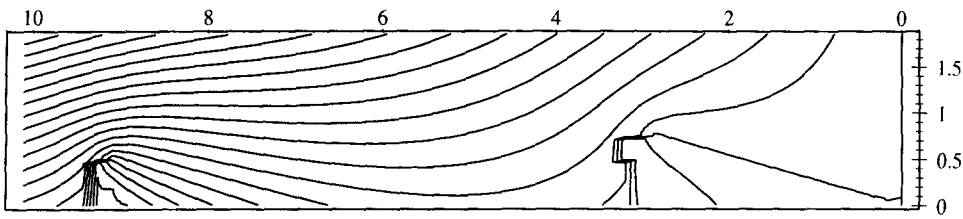

Fig. 4. A contour plot of $\mathrm{Im}(F(r))$ as obtained from the basic TBA equations (1.5)–(1.9), with r lying in the box $0 \leqslant \mathrm{Re}(r) \leqslant 1.85$, $0 \leqslant \mathrm{Im}(r) \leqslant 10.1$, showing the branch points at r_0 and r_1, and also the segment of the negative-λ line, running from 0 to r_0, along which $\mathrm{Im}(F(r)) = 0$. The box was scanned from right to left, so the lower branch of this segment is visible.

the quasiprimary fields at level 5 and including as many derivative states as the program allowed. The discrepancies are too small to see on the figure, being of order 10^{-9} at small values of r, growing to 10^{-3}–10^{-4} (depending on the level of the state) at $r = 10$. The former errors can be traced to our numerics and should not be too hard to reduce, whilst the latter can be ascribed to truncation effects in the TCSA – in particular, they grow as the level of the state under consideration gets higher.

The only problem that the reader might notice is that the lowest set of points stops short, at $r \approx 2.53$. By this stage $\delta(r)$ has become so large that θ_0 has almost reached $\imath\pi/3$. We should expect trouble at such a point as a new kind of singularity enters into the equations, caused by singularities in $S(\theta-\theta_0)$ and $S(\theta-\overline{\theta}_0)$. We have tried to take this into account, but the resulting equation appears to be much less stable and has resisted our attempts at an iterative solution. We will return to this problem in Section 4; in any event it only appears to trouble the spin-zero state.

3. Two-particle states and beyond

The singularity at $r_0 = \rho_0 e^{5\pi\imath/12}$ is only the first of a whole sequence of singularities seen by the 'zero-particle' TBA (1.5)–(1.9). They are approximately evenly spaced along the direction of the imaginary axis: the next is at $r_1 \approx 0.5311+9.1346\imath$, and the next at $r_2 \approx 0.42+15.44\imath$. Fig. 4 shows the positions of r_0 and r_1, as emerged from the numerical solution of the basic TBA equations on a suitably fine grid.

On the analytical side, we note that the first iterative correction to the Ising-like behaviour of (1.5), namely $\phi * \log(1+e^{-r\cosh\theta})$, tends uniformly to zero as $\mathrm{Im}(r) \to \pm\infty$ with $\mathrm{Re}(r) > 0$ held fixed.[3] Hence we expect that the locations of the r_n will eventually approach $(2n+1)\pi\imath$ as $n \to \infty$. These appear to be the only branch points on that part of the Riemann surface of $F(r)$ explored by the zero-particle TBA. However, the full surface must have much more structure: the behaviour of the action (1.4) under $\lambda \to \overline{\lambda}$ means that each singularity r_n beyond the symmetrically placed r_0 must have an image on some other sheet, located at

[3] when checking this, it is helpful to note that $\int_0^{2\pi} \log(1+\alpha e^{\imath\gamma})\,d\gamma = 0$ for $|\alpha| < 1$.

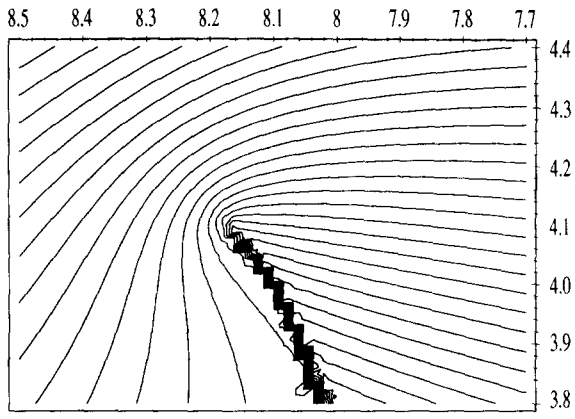

Fig. 5. $\mathrm{Im}(F(r))$ in the box $3.8 \leqslant \mathrm{Re}(r) \leqslant 4.4$, $7.7 \leqslant \mathrm{Im}(r) \leqslant 8.5$ as obtained from the one-particle TBA equations (2.3), (2.4), showing the branch point at $\tilde{r}_1$.

$$\tilde{r}_n \equiv e^{5\pi\imath/6}\bar{r}_n \,. \tag{3.1}$$

These images, invisible to the zero-particle TBA, should instead be seen by the more general TBA systems that we are trying to construct.

This idea is confirmed by the values of $F(r)$ which result from the one-particle TBA introduced in the last section: a grid plot of its real and imaginary parts exhibits a square root singularity at $\tilde{r}_1 \approx 4.1074{+}8.1763\imath$. An example of such a plot is shown in Fig. 5. (Incidentally, that this works is a further piece of support for the results of the last section.) Judicious use of the TCSA, allied with TBA data as a check on accuracy, is a great help in mapping out how the various sheets fit together, and seems to be qualitatively reliable at least out to $|r| = 20$. Here, it tells us that the branch point at $\tilde{r}_1$ should connect with the first two-particle state. We can therefore play the same game as before, and study the behaviour of the solution $\varepsilon(\theta)$ of the one-particle TBA as r is continued round $\tilde{r}_1$. This should yield a two-particle TBA equation.

When r approaches the branch point, we found that the singularities at $\theta = \pm\theta_0$, already implicated in the one-particle equation, remained near $\pm\imath\pi/6$, whilst a second pair headed for the real axis, just as happened when the one-particle TBA was being formed. Strictly speaking we should now repeat the rest of the one-particle work, this time keeping track of two independent singularity positions, θ_0 and θ_1, as r returns to the real axis. Numerically this is delicate: with both θ_0 and θ_1 to locate, an efficient iteration scheme is hard to find, and so we will leave this question to one side for the time being. Besides, in some respects the key piece of information has already been obtained: the two-particle TBA equation should involve four singularity terms, tied to singularities in $L(\theta)$ at $\pm\theta_0$ and $\pm\theta_1$. Once r reaches the real axis, the situation changes favourably: we expect the four singularities to be invariant not only under $\theta_i \to -\theta_i$, but also under $\theta_i \to \bar{\theta}_i$. This reduces to one the number of independent singularity positions, making a numerical solution no harder than the cases examined in the last section. The TBA equation to solve reads

$$\varepsilon(\theta) = r\cosh\theta + \log\frac{S(\theta-\theta_0)}{S(\theta-\bar{\theta}_0)} + \log\frac{S(\theta+\bar{\theta}_0)}{S(\theta+\theta_0)} - \phi * L(\theta)\,,$$

$$c(r) = \imath\frac{12r}{\pi}(\sinh\theta_0 - \sinh\bar{\theta}_0) + \frac{3}{\pi^2}\int_{-\infty}^{\infty} d\theta\, r\cosh\theta L(\theta)\,, \tag{3.2}$$

with θ_0 satisfying

$$\varepsilon(\theta_0) = (2n+1)\imath\pi\,. \tag{3.3}$$

For the lowest two-particle state, found on continuing round $\tilde{r}_1$, we found $\varepsilon(\theta_0) = \imath\pi$, so that n is equal to zero. However, the results of the last section make it very natural to allow for the more general possibility, in the hope of catching the other two-particle states. As with the one-particle TBA equation (2.8), θ_0 and $\bar{\theta}_0$ cease to be complex conjugate if r strays from the real axis, eventually metamorphosing into θ_0 and $-\theta_1$ as $\tilde{r}_1$ is approached.

The analysis of the infrared limit proceeds in much the same way as for the $s \neq 0$ one-particle states. Substituting $\theta = \theta_0$ in the first of (3.2) and taking the imaginary part of the large-r asymptotic gives us

$$2\pi(2n + \tfrac{1}{2}(1-\mathrm{sign}(\delta(r)))) \sim r\sinh(\mathrm{Re}(\theta_0)) + 2\mathrm{Im}\log\frac{S(\theta_0+\bar{\theta}_0)}{S(2\theta_0)}\,, \tag{3.4}$$

where, as before, $\mathrm{Im}(\theta_0) = \pi/6 + \delta(r)$ and $\delta(r) \to 0$ as $r \to \infty$. In the functions S, $\delta(r)$ can be replaced by its limiting value, so these terms become

$$\mathrm{Im}\log S(2\mathrm{Re}(\theta_0) + \imath\pi/3) = \tfrac{1}{2}\mathrm{Im}\log S(2\mathrm{Re}(\theta_0)) \tag{3.5}$$

(using the ϕ^3 property of $S(\theta)$) and

$$\mathrm{Im}\log S(2\mathrm{Re}(\theta_0)) = -\imath\log S(2\mathrm{Re}(\theta_0))\,. \tag{3.6}$$

(Recall that $S(\theta)$ is a pure phase for θ real, so the right-hand side of (3.6) is indeed real.) Combining all of these terms together, (3.4) becomes

$$2\pi(2n + \tfrac{1}{2}(1-\mathrm{sign}(\delta(r)))) \sim r\sinh(\mathrm{Re}(\theta_0)) - \imath\log S(2\mathrm{Re}(\theta_0))\,. \tag{3.7}$$

This is just the Bethe ansatz quantisation condition for a two-particle state with rapidities $(-\mathrm{Re}(\theta_0), \mathrm{Re}(\theta_0))$ and Bethe quantum numbers

$$\left(-2n+\tfrac{1}{2}\mathrm{sign}(\delta), 2n-\tfrac{1}{2}\mathrm{sign}(\delta)\right) = \left(-\frac{1}{2},\frac{1}{2}\right), \left(-\frac{3}{2},\frac{3}{2}\right), \left(-\frac{5}{2},\frac{5}{2}\right)\ldots \tag{3.8}$$

with $n = 0, 1, 1, 2, 2, \ldots$ and $\mathrm{sign}(\delta) = -1, 1, -1, \ldots$. (see, for example, Eq. (4.5) of Ref. [10]). These values of $\mathrm{sign}(\delta)$ should be imposed when handling the equation numerically, so that when seeking to follow a particular solution, the idea is to specify not only the value of $\varepsilon(\theta_0)$, Eq. (3.3), but also the sign of $\delta(r)$. The only point where we were not able to impose a particular sign on δ and obtain reasonable results was when we attempted to set $\mathrm{sign}(\delta) = +1$ when n in (3.3) is equal to zero. From a

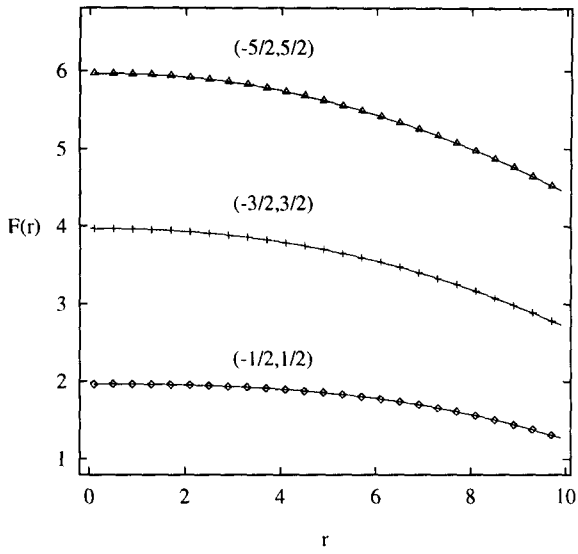

Fig. 6. Proposed zero-momentum two-particle scaling functions (points) compared with TCSA data (continuous lines).

physical point of view, this is as it should be, given the exclusion principle – otherwise, the state $(-\frac{1}{2}, \frac{1}{2})$ would have appeared twice.

Substituting the value of $\mathrm{Re}(\theta_0)$ which follows from (3.8), together with $\mathrm{Im}(\theta_0) = \pi/6$, into (3.2) automatically gives the expected algebraic asymptotic for $F(r)$. The next section will examine the ultraviolet limits analytically; in the meantime Fig. 6 illustrates the numerical agreement with TCSA data for the first three states. The discrepancies were much the same as for the one-particle sector, described earlier.

By this point the structure is clear enough that we can conjecture a general equation for an n-particle state:

$$\varepsilon(\theta) = r\cosh\theta + \sum_i \log\frac{S(\theta-\theta_i)}{S(\theta-\bar{\theta}_i)} - \phi * L(\theta)\,,$$

$$c(r) = \iota\sum_i \frac{6r}{\pi}(\sinh\theta_i - \sinh\bar{\theta}_i) + \frac{3}{\pi^2}\int_{-\infty}^{\infty} d\theta\, r\cosh\theta L(\theta)\,, \tag{3.9}$$

We expect that particular states are selected by imposing the values of $\varepsilon(\theta_i)$, and also the signs of the various δ_i. We only analysed in detail the spin-zero three-particle states, where steps similar to those already described give the following Bethe ansatz quantum numbers:

$$(-2n + \tfrac{1}{2} + \tfrac{1}{2}\mathrm{sign}(\delta), 0, 2n - \tfrac{1}{2} - \tfrac{1}{2}\mathrm{sign}(\delta)) = (-1,0,1), (-2,0,2), \ldots \tag{3.10}$$

with $n = 1,1,2,2,3\ldots$ and $\mathrm{sign}(\delta) = +1,-1,+1,\ldots$ Again, the exclusion principle leads us to suppose that the $n = 0$ case should be omitted.

This large-r asymptotic, together with the special cases already studied in some detail, lend support to (3.9). However, numerical work will also be needed. In particular, the equation will have to be modified at values of r below some critical r_c whenever the phenomenon observed above for the spin-zero one-particle state occurs, and the imaginary part of a singularity position θ_i ventures too far from $\pi/6$. We suspect that this will happen whenever one of the Bethe ansatz quantum numbers is equal to zero, and thus will afflict the three-particle states just discussed. In fact there are signs that this is just what is needed to get the ultraviolet asymptotics correct in these cases, a point that we shall return to later.

4. Ultraviolet behaviour

Analytic work has thus far been restricted to the infrared regime. In this section the opposite limit is considered, and the ultraviolet scaling dimensions of various states extracted. We start with the two-particle states.

In the limit $r \to 0$, the two-particle TBA splits into a pair of kink systems, just as for the ground state. For the right kink system, the terms from the singularities at $-\theta_0$ and $-\bar{\theta}_0$ drop out, and $r\cosh\theta$ can be replaced by $\frac{1}{2}re^{\theta}$. The real part of θ_0 tends to infinity like $\log(1/r)$; we will also need a little information about the behaviour of the imaginary part. Recall that for large r, $\mathrm{Im}(\theta_0) \sim \pi/6+\delta(r)$ with $\delta(r) \to 0$ as $r \to \infty$. In the opposite direction, we find that, although $\delta(r)$ grows, it tends to a finite and still-small limit as $r \to 0$. The precise value drops out of the final equations; the only important fact is that for all of the two-particle states (and also for all of the $s \neq 0$ one-particle states) its absolute value is less than $\pi/6$. Quite why this is important should become clear shortly. The scale-invariant kink TBA reads

$$\varepsilon(\theta) = \frac{r}{2}e^{\theta} + \log\frac{S(\theta-\theta_0)}{S(\theta-\bar{\theta}_0)} - \phi * L(\theta)\,. \tag{4.1}$$

(Note, to pass from this 'chiral' TBA equation to the general one-particle equation introduced in Section 2, we just need to replace $\frac{1}{2}e^{\theta}$ with $\cosh\theta$.) Next, eliminate r by replacing θ with $\theta - \log r$ and $\varepsilon(\theta)$ by $\varepsilon(\theta - \log r)$, to find

$$\varepsilon(\theta) = \tfrac{1}{2}e^{\theta} + \log\frac{S(\theta-\eta)}{S(\theta-\overline{\eta})} - \phi * L(\theta)\,, \tag{4.2}$$

where $\eta = \theta_0 + \log r$. In terms of these quantities, the limiting value of $c(r)$ is

$$c = \frac{3}{\pi^2}\int_{-\infty}^{\infty} d\theta\, e^{\theta} L(\theta) + \frac{6}{\pi}\,\iota\,(e^{\eta} - e^{\overline{\eta}})\,. \tag{4.3}$$

Now we proceed in the usual manner. First take a derivative with respect to θ:

$$\frac{\partial}{\partial\theta}\varepsilon(\theta) = \tfrac{1}{2}e^{\theta} + \frac{\partial}{\partial\theta}\log\frac{S(\theta-\eta)}{S(\theta-\overline{\eta})} - \frac{\partial}{\partial\theta}\phi * L(\theta)\,. \tag{4.4}$$

Now substitute this into the formula for c:

$$c = \frac{6}{\pi^2}\int_{-\infty}^{\infty} d\theta L(\theta)\frac{\partial}{\partial\theta}\left(\varepsilon(\theta) - \log\frac{S(\theta-\eta)}{S(\theta-\overline{\eta})} + \phi * L(\theta)\right) + \frac{6}{\pi}\iota\,(e^{\eta} - e^{\overline{\eta}}). \quad (4.5)$$

Then (remembering that $\phi(\theta) = -\iota\frac{\partial}{\partial\theta}\log S(\theta)$)

$$c = \frac{6}{\pi^2}\left[\int_{\varepsilon_{\min}}^{\varepsilon_{\max}} dx\,\log(1+e^{-x}) + \frac{1}{2}\varepsilon_{\min}\log(1+e^{-\varepsilon_{\min}})\right] - \frac{6}{\pi}\iota\left[2\phi * L(\eta) - 2\phi * L(\overline{\eta}) - e^{\eta} + e^{\overline{\eta}}\right]. \quad (4.6)$$

The first piece can be expressed in terms of the Rogers' dilogarithm function

$$\mathcal{L}(z) = -\tfrac{1}{2}\int_0^z dt\left(\frac{\log(1-t)}{t} + \frac{\log t}{1-t}\right)$$

as

$$\frac{6}{\pi^2}\left[\mathcal{L}\left(\frac{1}{1+e^{\varepsilon_{\min}}}\right) - \mathcal{L}\left(\frac{1}{1+e^{\varepsilon_{\max}}}\right)\right], \quad (4.7)$$

whilst the second can be evaluated using (4.2) for η and $\overline{\eta}$:

$$\begin{aligned} 2n\pi\iota &= \tfrac{1}{2}e^{\eta} - \log(|S(\iota 2\mathrm{Im}(\eta))|) - \pi\iota\tfrac{1}{2}(1-\mathrm{sign}(\delta)) - \phi * L(\eta) \\ -2n\pi\iota &= \tfrac{1}{2}e^{\overline{\eta}} + \log(|S(\iota 2\mathrm{Im}(\overline{\eta}))|) + \pi\iota\tfrac{1}{2}(1-\mathrm{sign}(\delta)) - \phi * L(\overline{\eta}), \end{aligned} \quad (4.8)$$

and is equal to $12(4n+1-\mathrm{sign}(\delta))$.

Finally, $\varepsilon_{\min}$ is reached as $\theta \to -\infty$, $\varepsilon_{\max}$ as $\theta \to \infty$. Since $S(\pm\infty) = 1$, the limiting form of (4.1) gives $\varepsilon_{\min} = \log((1+\sqrt{5})/2)$ and $\varepsilon_{\max} = \infty$, a result which was also checked against our numerical solutions. Since $\mathcal{L}(2/(3+\sqrt{5})) = \pi^2/15$, this gives us

$$c = \frac{2}{5} - 12(4n + 1 - \mathrm{sign}(\delta)). \quad (4.9)$$

The calculation for the $s \neq 0$ one-particle states is essentially identical. The only difference is that one of the two kink systems is in its 'ground state', in that there are none of the extra terms involving θ_0. Hence the size of the additional contribution is halved, and

$$c = \frac{2}{5} - 6(4n + 1 - \mathrm{sign}(\delta)). \quad (4.10)$$

Recalling from the infrared result (2.11) that $s = 2n+\frac{1}{2}(1-\mathrm{sign}(\delta))$, this is minus twelve times the scaling dimension on the cylinder of a spin s descendant of the primary field φ, as expected.

For $s = 0$ in the one-particle sector, the situation changes and our discussion must be much more tentative, as our numerical work lost stability below $r = r_c \approx 2.53$.

Nevertheless we can conjecture a plausible modification to the equation which seems to predict the correct ultraviolet asymptotic, and the remainder of this section is devoted to this question.

First, we must decide just how we expect the equation to change. In particular is important to know if the singularities at $\pm\theta_0$ stay on the imaginary axis, or if they somehow each split in two and acquire a real part. Unlikely as it appears at first sight, it seems that it is the latter possibility which actually occurs. One can gain information about this by again returning r into the complex plane, and following the position of θ_0 as r returns to points on the real axis below the critical value r_c. Padé extrapolation clearly showed a finite limiting value of $\mathrm{Re}(\theta_0)$ in each case we tried, the value increasing as the limiting r decreased. For example, extrapolating down from the upper half plane, we obtained $\mathrm{Re}(\theta_0) \approx 0.77$ at $r = 1.5$, and $\mathrm{Re}(\theta_0) \approx 1.17$ at $r = 1$. The extrapolation of $\mathrm{Im}(\theta_0)$ was not so reliable, but the results were consistent with the limiting value being $\pi/3$ every time. In any event, this seems to be the only way to make sense of the non-zero limit for the real parts, and so we will proceed on the assumption that indeed $\mathrm{Im}(\theta_0(r)) = \pi/3$ for all $r < r_c$.

When $\mathrm{Im}(\theta_0)$ finally reaches $\pi/3$, the singularities in $L(\theta)$ caused by the $\log S(\theta \pm \theta_0)$ term hit the real axis, forcing a deformation of the contour of integration. Integrating by parts in the convolution, and then taking the principal part to restore the contour to its original track, Eqs. (2.3), (2.4) should be modified thus:

$$\begin{aligned}
\varepsilon(\theta) &= r\cosh\theta + \log\frac{S(\theta-\theta_0)}{S(\theta+\theta_0)} + \tfrac{1}{2}\log\frac{S(\theta+(\theta_0-\imath\pi/3))}{S(\theta-(\theta_0-\imath\pi/3))} - \phi * L(\theta)\,,\\
c(r) &= \imath\frac{12r}{\pi}\sinh\theta_0 - \imath\frac{6r}{\pi}\sinh(\theta_0-\imath\pi/3)\\
&\quad + \frac{3}{\pi^2}\int_{-\infty}^{\infty} d\theta\, r\cosh\theta L(\theta)\,,
\end{aligned} \tag{4.11}$$

The factors of $1/2$ appear because the singularities remain on the real axis. This equation looks rather complicated, but simplifies once we put $\theta_0 = \beta + \imath\pi/3$, with β real. Using the bootstrap equation we find

$$\begin{aligned}
\varepsilon(\theta) &= r\cosh\theta + \tfrac{1}{2}\log\frac{S(\theta-\beta-\imath\pi/3)}{S(\theta-\beta+\imath\pi/3)} + \tfrac{1}{2}\log\frac{S(\theta+\beta-\imath\pi/3)}{S(\theta+\beta+\imath\pi/3)} - \phi * L(\theta)\,,\\
c(r) &= -\frac{6r}{\pi}\sqrt{3}\cosh\beta + \frac{3}{\pi^2}\int_{-\infty}^{\infty} d\theta\, r\cosh\theta L(\theta)\,.
\end{aligned} \tag{4.12}$$

To understand what has happened, it is worth thinking about how the 'singular values' of $\varepsilon(\theta)$ have moved around. This can be discussed using the functions $Y(\theta) \equiv e^{\varepsilon(\theta)}$ which solve, for the Lee–Yang model, the following functional equation or Y-system [11]

$$Y(\theta-\imath\frac{\pi}{3})\,Y(\theta+\imath\frac{\pi}{3}) = 1 + Y(\theta)\,. \tag{4.13}$$

The special points that we are interested in, θ_0 being an example, are those for which $1+Y=0$. Given such a point $\theta^{(0)}$, the Y-system can be used to find a sequence of other points $\theta^{(k)} \equiv \theta^{(0)}+k\pi\imath/3$ where Y also takes special values. Setting $Y^{(k)} = Y(\theta^{(k)})$, with $Y^{(k+5)} = Y^{(k)}$ by the periodicity of the Y-system, the sequence cycles round as $-1, A, B, -1, 0$, with $A+B = 0$ and $Y^{(0)}$ either the first or the fourth term. For θ_0, the former option is realised and so as θ_0 moves around, it carries with it the points $\theta_0-\imath\pi/3$ and $\theta_0-2\imath\pi/3$, at which Y takes the values 0 and -1, respectively. While $r > r_c$, these points lie on the imaginary axis, together with a symmetrically placed triplet of points associated with $-\theta_0$. When r reaches r_c, the points $\theta_0-2\imath\pi/3$ and $-\theta_0$ collide at $-\imath\pi/3$. Since for both of these points $1+Y = 0$, this opens up another possibility to distort the singularity positions while maintaining the symmetry under $\theta \to \bar{\theta}$ that they must respect while r remains real. This seems to be realised here: as r decreases below r_c, the points $\theta_0 - 2\imath\pi/3$ and $-\theta_0$ move away parallel to the real axis, with a similar story at $+\imath\pi/3$ ensuring that the symmetry is preserved. By continuing r away through complex values, we were able to observe this end result without having to tangle with the particularly singular behaviour actually at $r = r_c$.

The last task is to find an equation for θ_0, or equivalently for β. The value of $\varepsilon(\theta_0)$ remains equal to $\imath\pi$, but one must be careful when substituting $\theta = \theta_0$ into the first of (4.12). This is because the singularities just discussed cause the right-hand side of this equation to develop a couple of singularities precisely when $\theta = \theta_0$. Of course, the overall result remains finite, and the simplest approach seems to be to consider the limit of $\varepsilon(\beta+\imath\pi/3-\imath\epsilon) - \varepsilon(\beta-\imath\pi/3+\imath\epsilon)$ as $\epsilon \to 0^+$. From one point of view this is equal to $2\imath\pi$; equating this with the result from the right-hand sides we found

$$\imath\pi = \imath\sqrt{3}\, r \sinh\beta + \frac{1}{2}\log\frac{S(2\beta)}{S(2\beta+\imath 2\pi/3)}\frac{S(2\beta)}{S(2\beta-\imath 2\pi/3)} - (\phi * L(\beta+\imath\pi/3) - \phi * L(\beta-\imath\pi/3)) . \tag{4.14}$$

(We should mention here that we have been somewhat cavalier throughout in our treatment of the branch choices for the logarithms. This issue deserves a careful study, especially in regard to the way the branches behave under analytic continuation between energy levels.)

This concludes the modifications to the one-particle equation. If the comment made at the end of Section 3 is correct, then a similar manœuvre will be needed whenever a zero-momentum particle is present in a Bethe ansatz state. The natural generalisation of the equations just obtained for such situations, correcting Eq. (3.9) for r less than some r_c, is

$$\varepsilon(\theta) = r\cosh\theta + \tfrac{1}{2}\log\frac{S(\theta-\beta-\imath\pi/3)}{S(\theta-\beta+\imath\pi/3)}\frac{S(\theta+\beta-\imath\pi/3)}{S(\theta+\beta+\imath\pi/3)} + \sum_i \log\frac{S(\theta-\theta_i)}{S(\theta-\bar{\theta}_i)}\frac{S(\theta+\bar{\theta}_i)}{S(\theta+\theta_i)} - \phi * L(\theta) ,$$

$$c(r) = -\frac{6r}{\pi}\sqrt{3}\cosh\beta$$

$$+\imath\sum_i \frac{12r}{\pi}(\sinh\theta_i - \sinh\bar{\theta}_i) + \frac{3}{\pi^2}\int_{-\infty}^{\infty} d\theta\, r\cosh\theta L(\theta)\,, \tag{4.15}$$

where as above the singularity position θ_0 ceased to be purely imaginary at $r = r_c$, and was replaced in the equations by the real variable $\beta = \theta_0 - \imath\pi/3$.

Now we must analyse the $r \to 0$ limit. The first thing that we notice is that the modification has achieved the remarkable trick of splitting the 'zero-momentum' singularity position θ_0 into constituent singularities at $\imath\pi/3 \pm \beta$, which can now join the respective left and right kink systems. For the one-particle case, assuming that $\beta \to \infty$ as $r \to 0$, and replacing θ with $\theta - \log r$ and $\varepsilon(\theta)$ with $\varepsilon(\theta - \log r)$, the right-hand system becomes

$$\begin{aligned}\varepsilon(\theta) &= \tfrac{1}{2}e^{\theta} + \tfrac{1}{2}\log\frac{S(\theta-\eta-\imath\pi/3)}{S(\theta-\eta+\imath\pi/3)} - \phi * L(\theta)\,,\\ c &= -\frac{3}{\pi}\sqrt{3}\,e^{\eta} + \frac{3}{\pi^2}\int_{-\infty}^{\infty} d\theta\, e^{\theta}L(\theta)\,,\end{aligned} \tag{4.16}$$

where $\eta = \beta + \log r$ satisfies the 'quantisation condition'

$$\imath\pi = \imath\frac{\sqrt{3}}{2}e^{\eta} - \left(\phi * L(\eta + \imath\pi/3) - \phi * L(\eta - \imath\pi/3)\right)\,. \tag{4.17}$$

Now the calculation runs as before, modulo one subtlety to be mentioned shortly. One finds

$$\begin{aligned}c = &-\frac{3\sqrt{3}}{\pi}\,e^{\eta} + \frac{6}{\pi^2}\left[\int_{\varepsilon_{\min}}^{\varepsilon_{\max}} dx\,\log(1+e^{-x}) + \tfrac{1}{2}\varepsilon_{\min}\log(1+e^{-\varepsilon_{\min}})\right]\\ &- \frac{6}{\pi}\imath\left[\phi * L(\eta+\imath\pi/3) - \phi * L(\eta-\imath\pi/3)\right]\,.\end{aligned} \tag{4.18}$$

Recognising the dilogarithm and using (4.17),

$$c = \frac{6}{\pi^2}\left[\mathcal{L}\left(\frac{1}{1+e^{\varepsilon_{\min}}}\right) - \mathcal{L}\left(\frac{1}{1+e^{\varepsilon_{\max}}}\right)\right] - 6\,. \tag{4.19}$$

As before, $\varepsilon_{\max} = \infty$, and $e^{\varepsilon_{\min}}$ solves $e^{2\varepsilon_{\min}} = 1 + e^{\varepsilon_{\min}}$, an equation which has two solutions:

$$e^{\varepsilon_{\pm}} = \frac{1 \pm \sqrt{5}}{2} \tag{4.20}$$

Previously we selected the positive solution, $\varepsilon(\theta)$ being a monotonically increasing real function in that case. However, this time note that $e^{\varepsilon(\infty)} = e^{\varepsilon_{\max}} = \infty$, and that as θ decreases along the real axis $e^{\varepsilon(\theta)}$ falls all the way down to zero at $\theta = \beta$. This suggests that the relevant solution by the time $\theta = -\infty$ is reached is the negative one (note, such solutions were previously observed to be of relevance to the excited states in some other

models by Martins, in Ref. [3]). The correct prescription for $\mathcal{L}(x)$ for general $x \in \mathbb{R}^+$ is (see for example Ref. [14])

$$\mathcal{L}(x) = \frac{\pi^2}{3} - \mathcal{L}(1/x) \quad \text{for } x > 1\,, \tag{4.21}$$

which in this case gives

$$\mathcal{L}(2/(3-\sqrt{5})) = \frac{\pi^2}{3} - \mathcal{L}(2/(3+\sqrt{5})) = \frac{4\pi^2}{15}\,. \tag{4.22}$$

This gives us $c = -22/5$, as expected for the spin-zero one-particle state, which in the ultraviolet is created by the identity operator I. (Note, the theory being non-unitary, this is *not* the ground state.) We also analysed the spin-zero three-particle sector, and found

$$c = -\frac{22}{5} - 12(4n+1-\mathrm{sign}(\delta)) \tag{4.23}$$

with $n = 1, 1, 2, 2, \ldots$ and $\mathrm{sign}(\delta) = +1, -1, +1, \ldots$ just as in the infrared. Note that here also n must start from 1: the two options at $n = 0$ give either $-22/5$, double-counting the state I, or $-22/5 - 24$, minus twelve times the would-be scaling dimension on the cylinder of the null field $\partial\bar{\partial}I$. This seems to suggest a relation between the exclusion principle on the Bethe ansatz quantum numbers, and the null field structure of the conformal states.

5. Conclusions

This work is still in its early stages. We would like to have a more secure understanding of the zero-momentum one-particle state, and in particular to be able to follow its behaviour numerically all the way down to $r = 0$. Work on this question is in progress. The situation for the remaining one-particle states, and for all of the two-particle states, is very satisfactory but beyond that our equations become more conjectural, albeit natural. Numerical and analytic work is needed, both to confirm their status and to unravel their structure. On the numerical side this poses the particular challenge of developing efficient methods for the tracking of a number of singularities simultaneously, but this should not be insurmountable – the three-particle state would be a good starting point. Quite apart from the analytic insights we can hope for, the method promises to be very competitive numerically with the TCSA, particularly for higher levels and larger values of r. Note also that all of the results we have obtained for the SLYM are directly relevant, after a multiplication by two, to the thermally perturbed three-state Potts model. This follows from the simple relationship between their respective ground-state TBA systems [1].

Turning to more general issues, many new features of the TBA equations seem to emerge when the whole complex r plane is considered, and there remains much to explore. The map $\lambda \to \bar{\lambda}$, simple in its effects from the point of view of the perturbative action (1.4), is far from trivial when acting through Eq. (3.1), as $r \to \tilde{r}$, on the space of

multiparticle TBA equations. More locally in this space, the study of the zero, one and two particle TBA systems has shown how one equation can melt into another with the passage of singularities across the real axis, and it is important to extend this treatment further. An immediate hope would be to thereby justify the more general equations (3.9) conjectured above. In addition, given the good understanding of the ultraviolet and infrared limits of the model provided by conformal field theory and the Bethe ansatz quantisation conditions respectively, one might try to say something about the structure of the full Riemann surfaces for $F(r)$ in the various sectors, and to understand the way in which the domains of the various TBA equations are patched together on these surfaces.

We would like to stress how general the method advocated in this paper should be. As a first step, there seems to be no serious obstacle to its application to the known purely elastic scattering theories. In the absence of any numerical work to report at this stage, we will restrict ourselves to a couple of comments. First, we note the crucial rôle that the ϕ^3 property of $S(\theta)$ played in much of the analysis presented above. One can anticipate that other cases will exhibit a similar interplay between the algebraic properties of the S-matrix and the asymptotics of the multiparticle TBA equations. Second, many scattering theories, purely elastic and otherwise, exhibit additional symmetries which on the one hand divide the Hilbert space into further subsectors, and on the other permit the construction of alternative 'seed' TBA [4]. These will provide additional starting points for the continuation process, thus helping to fill out the extra sectors. In the Ising model example discussed in Section 1 this was exactly how the states related to the spin field arose.

Our main conclusion, however, is rather more ambitious than this. It is that *any* ground-state TBA equation encodes within itself equations for many excited states, and that analytic continuation provides the means by which these equations can be extracted. It will be interesting to see just how far this programme can be carried through.

Acknowledgements

We would like to thank Francesco Ravanini for some very useful discussions in the early stages of this project. We are also grateful for comments and help at various points from Carl Bender, Elena Boglione, Kevin Thompson and Mathew Penrose. P.E.D. thanks the EPSRC for an Advanced Fellowship, and R.T. thanks the Mathematics Department of Durham University for a postdoctoral fellowship. This work was supported in part by a Human Capital and Mobility grant of the European Union, contract number ERBCHRXCT920069, and in part by a NATO grant, number CRG950751.

Note added

Ref. [15], by Bazhanov et al., appeared as we were finishing this paper. These authors independently obtained TBA-like equations for the spin-zero excited states of the SLYM, though by a very different route from the one that we have described here.

References

[1] Al.B. Zamolodchikov, Thermodynamic Bethe Ansatz in Relativistic Models. Scaling 3-state Potts and Lee–Yang Models, Nucl. Phys. B 342 (1990) 695.
[2] T.R. Klassen and E. Melzer, Spectral flow between conformal field theories in (1+1) dimensions, Nucl. Phys. B 370 (1992) 511.
[3] M.J. Martins, Complex excitations in the thermodynamic Bethe ansatz approach, Phys. Rev. Lett. 67 (1991) 39.
[4] P. Fendley, Excited state thermodynamics, Nucl. Phys. B 374 (1992) 667.
[5] C.M. Bender and T.T. Wu, Anharmonic oscillator, Phys. Rev. 184 (1969) 1231.
[6] T.R. Klassen and E. Melzer, The thermodynamics of purely elastic scattering theories and conformal perturbation theory, Nucl. Phys. B 350 (1991) 635.
[7] V.A. Fateev, The exact relations between the coupling constants and the masses of particles for the integrable perturbed conformal field theories, Phys. Lett. B 324 (1994) 45.
[8] J.L. Cardy and G. Mussardo, S matrix of the Yang-Lee edge singularity in two-dimensions, Phys. Lett. B 225 (1989) 275.
[9] R.J. Eden, P.V. Landshoff, D.I. Olive and J.C. Polkinghorne, The analytic S-matrix (Cambridge Univ. Press, Cambridge, 1966).
[10] V.P. Yurov and Al.B. Zamolodchikov, Truncated conformal space approach to the scaling Lee–Yang model, Int. J. Mod. Phys. A 5 (1990) 3221.
[11] Al.B. Zamolodchikov, On the thermodynamic Bethe ansatz equations for the reflectionless ADE scattering theories, Phys. Lett. B 253 (1991) 391.
[12] M. Lüscher, Volume dependence of the energy spectrum in massive quantum field theories. 1. Stable particle states, Comm. Math. Phys. 104 (1986) 177;
T.R. Klassen and E. Melzer, On the relation between scattering amplitudes and finite-size mass corrections in QFT, Nucl. Phys. B 362 (1991) 329.
[13] M. Lässig and G. Mussardo, Hilbert space and structure constants of descendant fields in two-dimensional conformal theories, Computer Phys. Comm. 66 (1991) 71.
[14] A.N. Kirillov, Dilogarithm identities, Prog. Theor. Phys. Supp. 118 (1995) 61.
[15] V.V. Bazhanov, S.L. Lukyanov and A.B. Zamolodchikov, Integrable quantum field theories in finite volume: excited state energies, preprint CLNS 96/1416, LPM-96/24, hep-th/9607099 (July 1996).